

PACS numbers: 05.45.Df; 42.30.Ms; 87.64.Aa; 87.64.Cc
DOI: 10.1070/QE2011v041n04ABEH014570

The influence of the growth conditions of the plague microbe vaccine strain colonies on the fractal dimension of biospeckles

A.S. Ulianov, A.M. Lyapina, O.V. Ulianova, V.A. Fedorova, S.S. Ulianov

***Abstract*. Specific statistical characteristics of biospeckles, emerging under the diffraction of coherent beams on the bacterial colonies, are studied. The dependence of the fractal dimensions of biospeckles on the conditions of both illumination and growth of the colonies is studied theoretically and experimentally. Particular attention is paid to the fractal properties of biospeckles, emerging under the scattering of light by the colonies of the vaccinal strain of the plague microbe. The possibility in principle to classify the colonies of *Yersinia pestis* EV NIIEG using the fractal dimension analysis is demonstrated.**

Keywords: *speckle pattern, modelling, fractal dimension, Yersinia pestis EV NIIEG.*

1. Introduction

Fractals are complex geometrical figures, possessing the property of self-similarity [1]. In other words, a figure that has fractal properties, consists of several parts, each of which is similar (or approximately similar) to the whole figure.

Fractal structures often occur in nature and are studied in a variety of sciences. It is interesting to note that fractals occur in optics too in the case of speckle pattern formation under the light scattering in randomly inhomogeneous media or diffraction by rough surfaces.

It is usually assumed [2] that the transverse correlation function $C_\perp(r)$ of the spatial intensity fluctuations in a fractal speckle field is described by the expression

$$C_\perp(r) = r^{2(\mathscr{D}-2)},$$

where r is the spatial coordinate; $\mathscr{D}$ is the parameter varying in the interval $1 < \mathscr{D} < 2$. At the same time the longitudinal correlation function has the form [3]

$$C_\parallel(\Delta z) = \Delta z^{\mathscr{D}-2},$$

where Δz is the longitudinal distance (i.e., the distance along the optical axis of the system) between the adjacent points of observation of two speckle fields.

As already mentioned [4 – 13], the fractal properties of the speckle fields usually manifest themselves upon scattering by fractal structures. However, the fractal properties are also inherent in the patterns that arise under diffraction of ring beams (produced by axicons) by random inhomogeneous surfaces [14], or under double passing of a coherent beam through a random transparency [15].

In the opinion of the authors of the present paper (in the literature this question has not been discussed yet), the fractal properties should be inherent in the particular kind of structured speckle fields, referred in the English-language literature as compound speckles [16]. Such speckle fields arise when a random transparency is illuminated by two or more spatially separated beams of coherent light. The fractality of random optical fields may manifest itself also in a superposition of two or more cross-polarised statistically independent speckle patterns [17]. Optical fractals are often observed in scattering light by particle aggregates [18 – 20].

We should particularly mention the extremely interesting papers, devoted to the analysis of fractal speckle patterns, arising under the diffraction of tightly focused Gaussian beams, scanning randomly-inhomogeneous objects [21 – 23]. The mentioned patterns should be classified as one-dimensional optical fractals. Besides the one- and two-dimensional fractal fields, three-dimensional fractals also occur in optics. For example, the authors of [24] showed that an open curve drawn through the points of zero intensity of a 3D speckle field and having the minimal length may possess fractal properties.

In speckle optics the diffraction patterns, arising due to the scattering of coherent light by objects of biological origin, are often called biospeckles [25]. In analogy with these patterns, the optical fractals, formed due to the diffraction of radiation by biotissues, became to be referred as biofractal images [26] or simply biofractals [27].

In recent years the fractal structures found wide application in biology and medicine, from early diagnostics of cancer to revealing the susceptibility to schizophrenia [28 – 39]. Apparently, the most urgent problems are those associated with detecting pathogenic microorganisms in air or water environment, or with the identification of patho-

A.S. Ulianov, S.S. Ulianov N.G. Chernyshevsky National Research Saratov State University, ul. Astrakhanskaya 83, 410012 Saratov, Russia; e-mail: ulianovas@mail.ru;
A.M. Lyapina, V.A. Fedorova Saratov Research Veterinary Institute of the Russian Academy of Agricultural Sciences, ul. 53 Strelkovoi divizii 6, 1410028 Saratov, Russia;
O.V. Ulianova N.G. Chernyshevsky National Research Saratov State University, ul. Astrakhanskaya 83, 410012 Saratov, Russia; N.I. Vavilov Saratov State Agrarian University, Teatral'naya pl. 1, 410012 Saratov, Russia; e-mail: ulianovaov@mail.ru

Received 25 February 2011
Kvantovaya Elektronika **41** (4) 349 – 353 (2011)
Translated by V.L. Derbov

gens, extracted from infected animals or patients. The laser diagnostics of pathogenic bacteria has a long history (see, e.g. [40–43]). The methods of identification of microorganisms, based on light scattering, were approved on different bacteria, such as *Listeria spp*., *Stafilococus spp*., *Mycobacterium spp*., *Helicobacter pylori*, *Escherichia coli*, *Cryptosporidium parvum oocysts*, *Giardia lamblia*, and many others [44–54].

As recently found, the structure of some bacterial colonies strongly resembles complex fractals, which makes it possible to apply the methods of fractal analysis to the specific or intraspecific differentiation of bacteria [55]. However, as far as we know, up to date no attempts have been undertaken to develop methods for express-diagnostics and identification of pathogenic bacteria, based on the fractal analysis of biospeckles. Such methods could be extremely needed for detecting the agents of special danger infections, such as plague, at early stages of the disease.

The present paper partially fills this gap. Here we develop the fundamental base for express-diagnostics of the plague pathogenic agent (with the vaccinal strain *Yersinia pestis* EV NIIEG taken as a model) using the fractal analysis of speckle structures.

2. Theoretical study of the effect of the bacterial colonies illumination conditions on the fractal dimension of speckle patterns

In the numerical modelling it was assumed that the scattering object is located in the object plane of a microscope, while the observed speckle pattern is recorded in the image plane. If the imaging system allows resolution of all inhomogeneities of the scattering object, then the phase modulation in the object plane will not lead to additional amplitude modulation in the image plane. Therefore, the fractal dimension of the image should be exactly equal to that of the realisation of the sample function, describing the transmission coefficient of the bacterial cell colonies under observation.

However, the fractal dimensions of the object and its image may be different. First of all, this may be caused by the inhomogeneity of the illumination of the object by laser radiation. The centre of the illuminated colony may be shifted with respect to the centre of the laser beam cross section. In the experiment one should strive for the complete matching of the beam and colony size; however, in practice this condition is often not strictly satisfied. The bacterial colonies are incubated on Petri dishes (made of plastic or glass), filled with bacterial agar with the layer thickness of 4–5 mm. Both the agar and the Petri dish bottom are optically inhomogeneous objects, which introduce additional amplitude–phase modulation into the illuminating laser beam. If the colonies are illuminated not at right angle to the plane, in which the colony is located, or if the illuminating beam is defocused, then the interference fringes appear due to the influence of the plane-parallel plate, whose role is played by the bottom of the Petri dish. In addition, in the low-noise cameras with high spatial resolution an IR filter is usually mounted before the light-detecting element. Under certain illumination conditions with a helium–neon laser used as a source, the presence of the filter may cause the formation of oblique fringes with the period ~ 100 μm directly in the image plane.

Thus, the fractal dimension of the analysed images of bacterial colonies, recorded by the microscope camera under the coherent illumination, is measured with significant error. The latter may be caused by the formation of stripes (low contrast) or by the additional modulation due to the inhomogeneous illumination of the object. In the present Section we analyse the influence of the mentioned factors on the fractal dimension of the image. A Sierpinski carpet illuminated with a Gaussian beam is used as a test fractal object. As already mentioned, in the numerical modelling it was assumed that the resolution of the microscope is greater than the characteristic size of the spatial inhomogeneity of bacterial cell colonies. The influence of aberrations was also assumed inessential. Fractal dimensions of the obtained speckle patterns were calculated using the covering method. A more detailed description of this algorithm in application to the biospeckle analysis is presented in Ref. [56].

2.1 The influence of the illuminating beam diameter

The diameter D of grown-up colonies of the plague microbe (48 hours of incubation) is 2–3 mm. In the numerical experiments we analysed the fractal dimension of the images, obtained under the illumination of the 2×2 mm Sierpinski carpet with the Gaussian beam, whose diameter d varied from 0.5 to 2 mm with the step 170 μm. The structure of the object, illuminated with the Gaussian beam, is presented in Fig. 1 for three values of the parameter $R = d/D$.

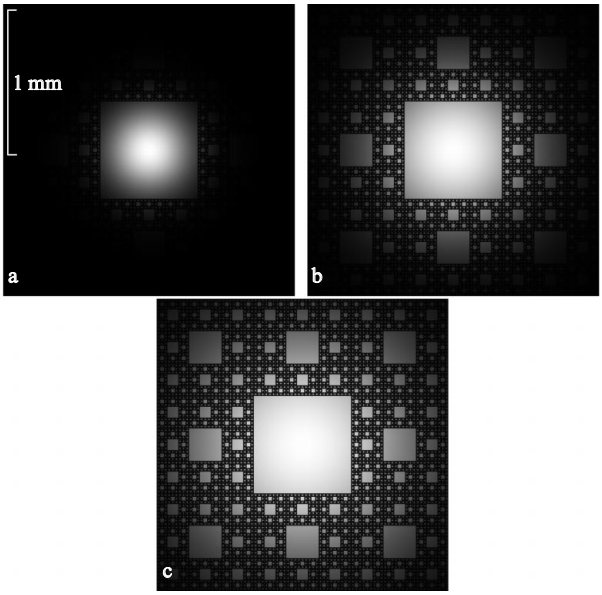

Figure 1. The structure of the fractal object (2×2 mm Sierpinski carpet) illuminated with a Gaussian beam at $R = 0.33$ (a), 0.66 (b), and 1 (c).

The results of the fractal dimension calculations are presented in Fig. 2, where the following notation is introduced: $s = \log_2 M$, $N(s) = \log_2 X$ (M and X are the size and the number of boxes, covering the image, respectively [56]), $\Delta N(s) = N(s_2) - N(s_1)$ with $s_2 - s_1 = \text{const}$ taken into account. The dependence of the fractal dimension, defined as $F = -N(s)/s$, on the parameter R is shown in Fig. 3a. It is seen that the fractal dimension of the image essentially depends on the relation between the beam diameter and that

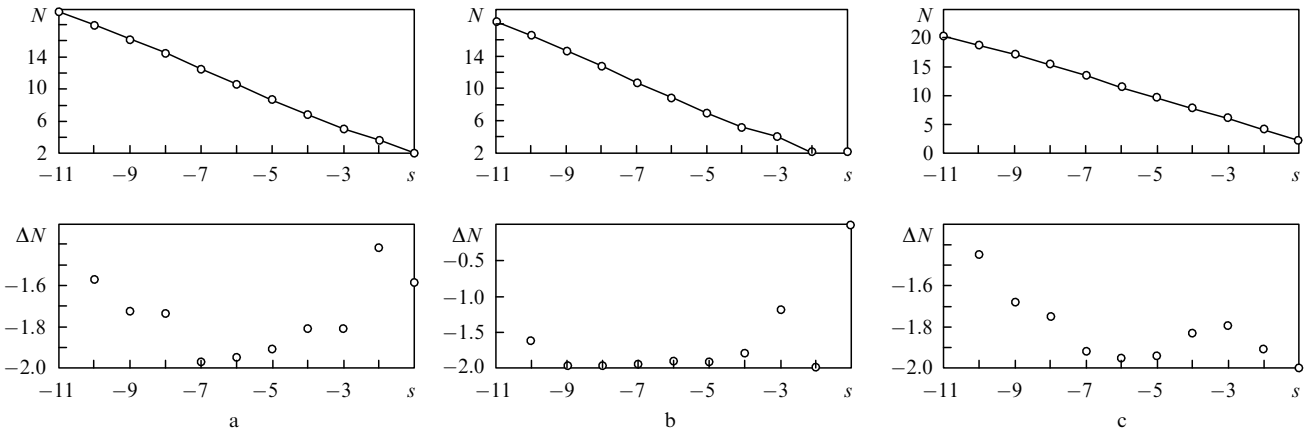

Figure 2. Dependences that determine the fractal dimension, obtained by numerical modelling at $R = 0.33$ (a), 0.66 (b), and 1 (c).

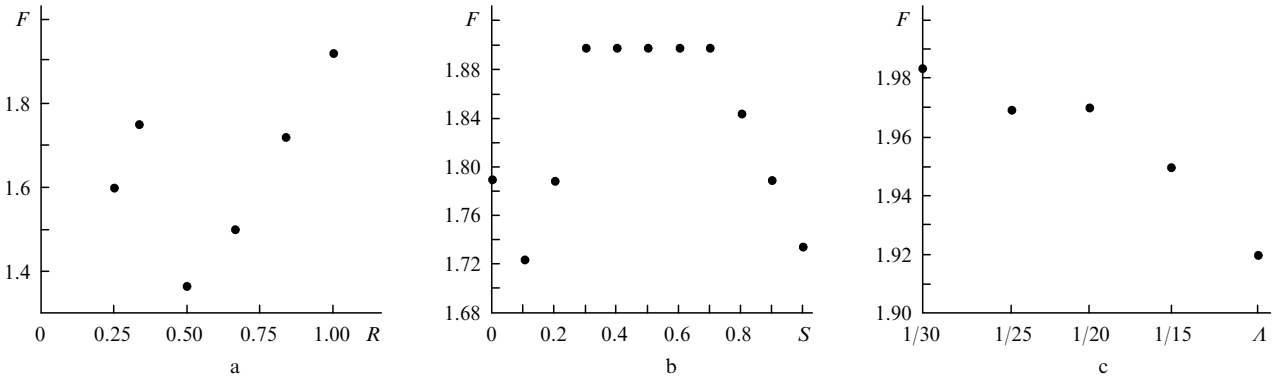

Figure 3. Dependences of the fractal dimension of the image on the parameter R (a), on the value of the displacement of the beam centre with respect to the object centre (b), and on the period of interference fringes, normalised to the characteristic size of the image.

of the fractal object under study. The character of the dependence is irregular, with a minimum in the vicinity of $R = 0.5$. The relative change in the fractal dimension may reach 15 %.

2.2 The influence of the illuminating beam position.

Based on the computer modelling, the dependence of the fractal dimension F on the position Δ of the centre of the illuminating beam with respect to the centre of the fractal object is studied. To characterise their relative displacement the quantity $S = \Delta/D$ was used. The dependence $F(S)$ is presented in Fig. 3b. It is seen that at large beam displacements ($S = 0.5$) the fractal dimension is changed by more than 8 %.

2.3 The influence of illumination inhomogeneity

To reveal the degree of the relation between the fractal structure of the image and the inhomogeneity of the object illumination, the incident beam was presented as a combination of a plane wave (dc component) and a Gaussian beam. The relative modulation depth $\sigma = I_{\text{gauss}}/I_{\text{plane}}$ was taken to serve as a measure of inhomogeneity, where I_{gauss} is the maximal value of the Gaussian beam intensity, and I_{plane} is the intensity of the plane wave. In the computer experiment σ was changed in the range 0.1 – 1.0 with the step 0.1. As the calculations show, the dependence of the fractal dimension on the modulation depth is absent, namely, $F(\sigma) = 1.87$ in the whole range of σ values.

2.4 The influence of the period of interference fringes

As already mentioned above, the image of the object may be modulated with fringes, formed due to the interference of light in the walls of the Petri dish or in the IR filter, covering the surface of the CMOS-camera. The period and the contrast of these fringes may be different. In the computer experiment the period Λ varied from 1/30 to 1/10 of the characteristic size of the image of the fractal object. The contrast of the fringes was taken equal to 1. The dependence $F(\Lambda)$ is illustrated in Fig. 3c. The relative change of the fractal dimension is not large (not greater than 1.5 %).

3. Experimental study of fractal properties of biospeckles, formed under the coherent illumination of the grow-up colonies of *Y. pestis* EV

3.1 Methods and materials

In the experiment we used the GN-5P He – Ne laser with the power 5 mW and the radiation wavelength 633 nm. The Gaussian laser beam with the diameter 1 mm was transformed into a collimated beam whose diameter was variable from 1 to 3 mm. The collimation was implemented using the system, comprising four lenses and an iris. The first part of the system comprised two lenses. The front focal plane of the second lens having the focal length 10 mm and the numerical aperture 0.55 (AL1210A, S-LAH64 Aspheric

Lens, Thorlab, USA) coincided with the back focal plane of the first lens having the focal length 1.14 mm and the numerical aperture 0.44 (C200TM-B, Thorlab, USA). This part of the collimating system served to form a broadened beam with the diameter 7 mm. The second part of the collimating system comprised two lenses having the focal length 1.14 mm and the numerical aperture 0.44 (C200TM-B, Thorlab, USA). The spatial filter, i.e., a small aperture with the diameter 5 μm (P5S, Thorlab, USA) was placed between the lenses in the plane of the beam focusing. All lenses and the spatial filter were mounted in two standard lens tubes (SM05L10, 0.5″ Lens Tube, Thorlab, USA) with the D5S iris (Thorlab, USA) mounted between them to match the diameter of the collimated beam with the characteristic size of the colonies.

To vary the illumination intensity, the rotary NDC-100C-4M attenuator (Mounted Continuously Variable ND Filter Thorlab, USA), i.e., a neutral filter whose optical density could vary in the range 0–4, was mounted before the collimating system. The collimated beam was targeted at the *Y. pestis* EV colony of interest by means of the ME05-M01 mirror (Gold, Thorlab, USA). The Petri dish was installed on the object stage of the Biolam microscope (LOMO, Russia). The monochrome digital WinCamD CMOS-camera (DataRay, USA) with the resolution 1024×1024 pixels was placed in the field-stop plane to record speckle patterns in the plane of the object image. To reduce the noise level of the speckle field detection we used the regime of averaging over 128 realisations. A characteristic speckle pattern, produced by illuminating the two-day-old colony of *Y. pestis* EV with the collimated laser beam, is shown in Fig. 4.

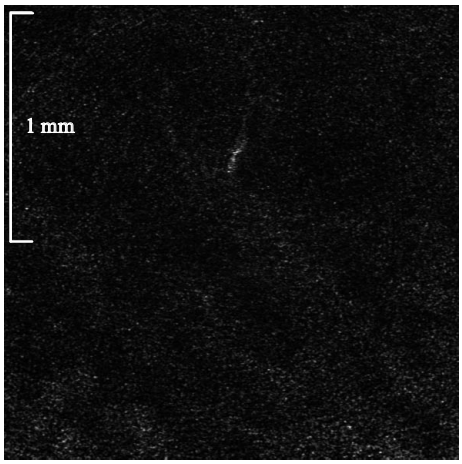

Figure 4. Speckle pattern obtained under the illumination of a two-day-old *Y. pestis* EV colony (incubated on the Hottinger agar) with a collimated laser beam.

The vaccinal strain *Y. pestis* EV was incubated on two commercial nutrient agars:

(i) 1.5 % BactoAgar with 2.5 % Heart Infusion Broth, pH 7.4 (Difco Laboratories, Detroit, Michigan, USA);

(ii) Hottinger agar with pH 7.4 (Russian Research Anti-Plague Institute 'Microbe', Saratov, Russia).

The photograph of a typical two-day-old colony of the plague microbe vaccine strain is presented in Fig. 5.

Two series of experiments were carried out. In the first of them the strain was incubated at the temperature $T = 26\,^{\circ}\mathrm{C}$ during 48 hours. In the second series the incubation was performed at $T = 26\,^{\circ}\mathrm{C}$ during 24 hours and then continued at $T = 37\,^{\circ}\mathrm{C}$ during the next 24 hours. The culture of the vaccinal strain *Y. pestis* EV was delivered by L.A. Tarasevich State Research Institute for Standardization and Control of Medical Biological Preparations, Moscow. The study was performed in the Research Bacteriologic Laboratory at the N.G. Chernyshevsky National Research Saratov State University.

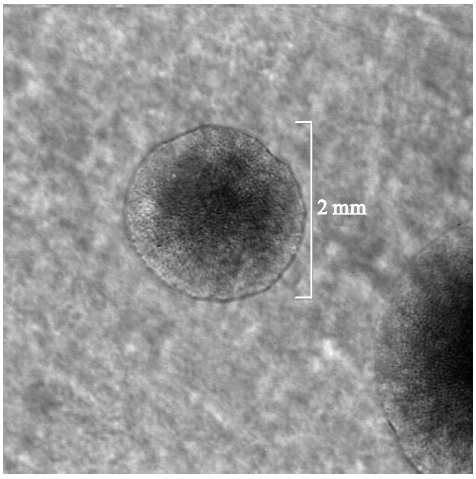

Figure 5. Photograph of the two-day-old *Y. pestis* EV colony (incubated on the Hottinger agar) under the illumination with white light.

3.2 Fractal dimension of biospeckles formed due to the scattering of coherent radiation by the *Y. pestis* EV bacterial colonies

Figure 6 presents the dependences that determine the fractal dimension of biospeckles, formed due to the diffraction of a coherent beam by the colonies, incubated under different conditions. In particular, the scattering by two-day-old colonies of *Y. pestis* EV, incubated on two agars at different temperatures, was studied. As the calculations show, the mean fractal dimensions for Figs 6a, b, c, and d are equal to 1.9, 1.96, 1.98, and 1.94, respectively. Keeping in mind that a change in the fractal dimension by 0.01 is significant, one may conclude that the biospeckles, produced by different colonies, possess different fractal structures.

4. Conclusions

The present paper shows that, in principle, it is possible to diagnose the changes in the conditions of the plague microbe colonies growth by calculating the fractal dimensions of the speckle patterns, arising under the illumination of the colonies with a Gaussian beam. The possibility of classification of the *Y. pestis* EV colonies using the analysis of the fractal dimension is also demonstrated. However, we should emphasise, that the method is extremely sensitive to the conditions of illumination and strongly affected by such factors as the formation of interference fringes in the walls of Petri dish. Correct evaluation of the biospeckles fractal dimension requires careful tuning and alignment of the microscope, which hampers wide application of the proposed method in the bacteriologic practice.

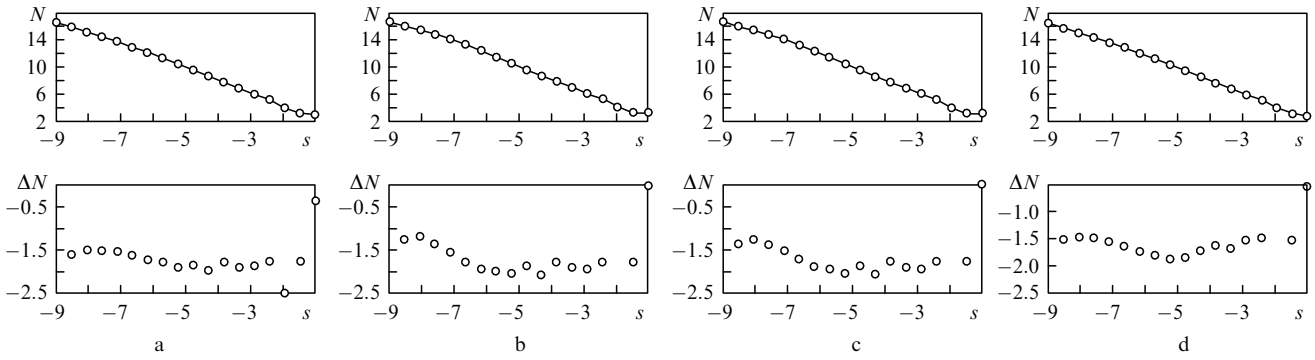

Figure 6. Dependences that determine the fractal dimension of biospeckles due to the scattering of light by bacterial colonies *Y. pestis* EV, incubated under different conditions: on the Hottinger agar at $T = 26\,^{\circ}\mathrm{C}$ during 48 hours (a), on the Hottinger agar at $T = 26\,^{\circ}\mathrm{C}$ during 24 hours followed by cultivating at $T = 37\,^{\circ}\mathrm{C}$ during the next 24 hours (b), on BactoAgar at $T = 26\,^{\circ}\mathrm{C}$ during 48 hours (c); on BactoAgar at $T = 26\,^{\circ}\mathrm{C}$ during 24 hours followed by cultivating at $T = 37\,^{\circ}\mathrm{C}$ during the next 24 hours.

Acknowledgements. The study was supported by the U.M.N.I.K. Programme, by the Ministry of Education and Science of the Russian Federation [Grant Nos 1.4.09 (2009 – 2010) and 2.1.1/4989 (2009 – 2010)], by the State Contract No. 02.740.11.0879 (2010), and also BII/ISTC No. 3853, and FRBAA 09-6G-1-0161.

References

1. Mandelbrot B. *The Fractal Geometry of Nature* (San Francisco: W.H.Freeman and Co., 1982).
2. Uozumi J., Ibrahim M., Asakura T. *Opt. Commun.*, **156**, 350 (1998).
3. Uozumi J. *Proc. SPIE Int. Soc. Opt. Eng.*, **4607**, 257 (2001).
4. Cheng C.F., Liu C.X., Teng S.Y. *Phys. Rev. E*, **65** (6), 061104 (2002).
5. Berry M.V. *J. Phys. A: Math. Gen.*, **12**, 781 (1979).
6. Jakeman E. *J. Phys. A: Math. Gen.*, **15**, L55 (1982).
7. Jakeman E. *Opt. Acta*, **30**,1207 (1983).
8. Jordan D.L., Hollins R.C., Jakeman E. *Appl. Phys. B*, **31**, 179 (1983).
9. Mendoza-Suarez A., Mendez E.R. *Appl. Opt.*, **36**, 3521 (1997).
10. Guerin C.A., Holschneider M., Saillard M. *Waves Random Media*, **7**, 331 (1997).
11. Sanchez-Gil J.A., Garcia-Ramos J.V., Mendez E.R. *Opt. Lett.*, **26**, 1286 (2001).
12. Uozumi J., Kimura H., Asakura T. *J. Mod. Opt.*, **38**, 1335 (1991).
13. Uno K., Uozumi J., Asakura T. *Opt. Commun.*, **124**, 16 (1996).
14. Uozumi J. *Proc. SPIE Int. Soc. Opt. Eng.*, **4705**, 95 (2002).
15. Uozumi J. *Proc. SPIE Int. Soc. Opt. Eng.*, **3904**, 320 (1999).
16. Hanson S.G., Jakobsen M.L., Hansen R.S., et al. *Proc. SPIE Int. Soc. Opt. Eng.*, **7008**, 70080M (2008).
17. Okamoto T., Fujita S. *J. Opt. Soc. Am. A*, **25** (12), 3030 (2008).
18. Khlebtsov N.G. *Opt. Spectrosc.*, **88** (4), 594 (2000).
19. Schmitt J.M., Kumar G. *Appl. Opt.*, **37** (13), 2788 (1998).
20. Wang R.K. *J. Mod. Opt.*, **47**, 103 (2000).
21. Zimnyakov D.A., Tuchin V.V. *Appl. Opt.*, **35**, 4325 (1996).
22. Tuchin V.V. *J. Biomed. Opt.*, **4**, 106 (1999).
23. Zimnyakov D.A. *Opt. Eng.*, **36** (5), 1443 (1997).
24. O'Holleran K., Dennis M.R., Flossmann F., et al. *Phys. Rev. Lett.*, **100**, 053902 (2008).
25. Aizu Y., Asakura T., in *Optics and Lasers in Biomedicine and Culture, OWLS – Optical Within Life Sciences* (Berlin: Springer, 2000) Vol. 5, pp 297 – 300.
26. Angelsky O.V., Ushenko A.G., Burkovets D.N., et al. *Proc SPIE Int. Soc. Opt. Eng.*, **4829**, 188 (2003).
27. Ushenko Yu.A., Kuritscin A.N. *Proc. SPIE Int. Soc. Opt. Eng.*, **4242**, 233 (2001).
28. Einstein A.J., Wu H.S., Gil J. *Phys. Rev. Lett.*, **80**, 397 (1998).
29. Bauer W. *Heavy Ion Phys.*, **14**, 39 (2001).
30. Hunter M., Backman V., Popescu G., et al. *Phys. Rev. Lett.*, **97**, 138102 (2006).
31. Pyhtila J.W., Ma H., Simnick A.J., et al. *J. Biomed. Opt.*, **11**, 034022 (2006).
32. Sboner A., Bauer P., Zumiani G., et al. *Skin Res. Technol.*, **10**, 184 (2004).
33. Kelloff G.J., Sullivan D.C., et al. *Cancer Biomarkers*, **3**, 1 (2007).
34. Brown W.J., Pyhtila J.W., Terry N.G., et al. *IEEE J. Sel. Top. Quantum Electron.*, **14**, 88 (2008).
35. Zhifand L., Hui L., Qiu Y. *Proc. SPIE Int. Soc. Opt. Eng.*, **6027**, 470 (2006).
36. Benhamou C.L., Poupon S., Lespessailles E., et al. *J. Bone Miner. Res.*, **16**, 697 (2001).
37. Pothuaud L., Lespessailles E., Harba R., et al. *Osteoporos. Int.*, **8**, 618 (1998).
38. Tosoni G.M., Lurie A.G., Cowan A.E., et al. *Oral Surgery, Oral Medicine, Oral Pathology, Oral Radiology, and Endodontology*, **102**, 235 (2006).
39. Ha T.H., Yoon U., Lee K.J., et al. *Neurosci. Lett.*, **384**, 172 (2005).
40. Wyatt P.J. *Nature*, **221**, 1257 (1969).
41. Stull V.R. *J. Bacteriology*, **109** (3), 1301 (1972).
42. Salzman G.C., Griffith J.K., Gregg C.T. *Appl. Env. Microbiology*, **44** (5), 1081 (1982).
43. Bronk B.V., van der Merwe W., Huffman D.R., in *Modern Techniques for Rapid Microbiological Analysis* (New York: VCH Publishers, 1992).
44. Devarakonda V., Manickavasagam S. *Proc. SPIE Int. Soc. Opt. Eng.*, **7306**, 73061B (2009).
45. Yeo C.B.A., Watson I.A., Wong J.W.M., et al. *Techn. Digest of European Conf. on Lasers and Electro-Optics* (Piscataway: IEEE, 1998).
46. Arizaga R., Gonzalez J.F., et al. *J. Biomed. Opt.*, **14**, 064015 (2009).
47. Krishnan A. et al., in *Food Processing Faraday, New Technologies for the Food Industry* (Melton Mowbray: Pera Innovation Park, 2004).
48. Bae E., Bai N., et al. *J. Biomed. Opt.*, **15** (4), 045001 (2010).
49. Bae E., Banada P.P., et al. *J. Biomed. Opt.*, **13** (1), 014010 (2008).
50. Bayraktar B. et al. *J. Biomed. Opt.*, **11** (3), 034006 (2006).
51. Stramski D. et al. *Proc. SPIE Int. Soc. Opt. Eng.*, **1750**, 73 (1992).
52. Bae E., Bai N., Aroonnual A. *Proc. SPIE Int. Soc. Opt. Eng.*, **7315**, 73150A (2009).
53. Katz A., Alimova A., Xu M. *Proc. SPIE Int. Soc. Opt. Eng.*, **4965**, 73 (2003).
54. Kotsyumbas I.Ya., Kushnir I.M., Bilyy R.O., et al. *Proc. SPIE OSA Biomed. Opt.*, **6631**, 66311I (2007).
55. Ulyanov A.S. *Opt. Spectrosc.*, **107** (6), 866 (2009).
56. Ulianov A.S. *Kvantovaya Electron.*, **38** (6), 557 (2008) [*Quantum Electron.*, **38** (6), 557 (2008)].